Tuning polymeric and drug properties in a drug eluting stent: a numerical study

Jahed Naghipoor[1,*], José A. Ferreira[2], Paula de Oliveira[2] and Timon Rabczuk[1]

[1]Institute of Structural Mechanics, Bauhaus-Universität Weimar, 99423, Weimar, Germany

[2]CMUC, Department of Mathematics, University of Coimbra, 3001-454, Coimbra, Portugal

Abstract

A two dimensional coupled nonlinear non-Fickian model for drug release from a biodegradable drug eluting stent into the arterial wall is studied. The influence of porosity and degradation of the polymer as well as the dissolution rate of the drug are analyzed. Numerical simulations that illustrate the kind of dependence of drug profiles on these properties are included.

Keywords: Domain decomposition methods, drug eluting stent, dissolved drug, numerical simulation

1 Introduction

Cardiovascular diseases are among the leading causes of death in the industrialized world. Although cardiovascular mortality rates have declined in many high-income countries, cardiovascular deaths have increased at a fast rate in low-income and middle-income countries ([17]). Among all cardiovascular diseases, atherosclerosis is the most common one wherein some arteries start thickening until they eventually occlude. The disease is characterized by intramural deposits of lipids and proliferation of vascular smooth muscle cells. These changes are accompanied by loss of elasticity of the vessel walls and narrowing of the vascular lumen. Coronary atherosclerosis is clinically the most important type of atherosclerosis. As coronary arteries are relatively narrow, atherosclerosis can seriously reduce the blood flow through them.

Over the past decade, arterial stents for scaffolding and expanding the narrowed coronary arteries, have evolved from the bare metal stents (BMS) to polymer coated drug-delivery vehicles and recently, fully biodegradable drug delivery configurations. BMS while revolutionary at the time,

---

*Corresponding author. Tel.: +49 3643 584512.

  E-mail: jahed.naghipoor@uni-weimar.de

were soon rendered unsatisfactory due to the relatively quick occurrence of the re-narrowing of the lumen (restenosis), as a result of the damage caused bt the stent to the endothelial cells of the arterial walls. To circumvent this drawback, the next generation of arterial stents, the drug-eluting stents (DES), included a therapeutic agent to prevent the occurrence of restenosis ([10]).

The DES, a device that releases an anti-proliferative drug with a programmed pharmacokinetics into the arterial wall, consists of a metallic stent strut coated with a polymeric layer that encapsulates a therapeutic drug. The drug reduces smooth muscle cell growth and prevents an inflammatory response which are the predominant causes of neointimal proliferation and in-stent restenosis.

Several studies showed that in the case of permanent-polymer based formulations, the influence of polymer-tissue interactions can induce severe host tissue responses, such as sub-acute thrombosis and in stent restenosis ([16]). Biodegradable polymers like polylactic acid (PLA) have become the materials of choice to coat the stents, the so called Drug Eluting Stents (DES), and to release the specific therapeutic agent to prevent thrombosis and in stent restenosis.

Arterial stiffness is considered as an excellent indicator of cardiovascular morbidity and mortality in a large percentage of the population as referenced in [9]. Taking into consideration the arterial stiffness in the mathematical modeling of drug release is a key factor to understand the pharmacokinetic of the drug in atherosclerosis. At low strains (physiological pressures), the media, the thickest tissue layer constituting the arterial wall, mainly determines the mechanical properties of the arterial wall. Moreover, due to the high content of smooth muscle cells compared to other layers, it is the media that is responsible for the viscoelastic behavior of the arterial wall. This aspect has been studied in ([6]), where to simplify the complex multi-layered structure of the arterial wall, only the interaction of the coated stent with media was considered.

When the plasma penetrates the biodegradable polymeric coating, it reacts with the polymer, producing diffusible molecules with smaller molecular weight. As the degradation proceeds the porosity of the polymer increases and consequently the effective diffusion coefficient of the drug molecules dispersed in the biodegradable polymer also increases ([18]). This time dependent porosity influences the pharmacokinetics of the drug and alters its residence time in the vessel wall. The interplay between porosity and degradation rate can act like a tuning mechanism to adapt the released drug concentration to a predefined profile. In the present paper we focus on that mechanism and we analyze its impact on the drug delivery in the vessel wall.

Domain decomposition method (DDM) is an efficient technique to solve multi-domain problems. It is used in this paper to simulate the polymer-wall problem. DDM solves an initial boundary value problem (IBVP) by splitting it into smaller IBVP on sub-domains and iterating the solution between adjacent sub-domains ([15]). We have considered a Robin-Robin domain decomposition algorithm to model the release of the degradation products and the dissolved drug into the arterial wall.

The paper is organized as follows. In Section 2, the nonlinear non-Fickian coupled cardiovascular model is introduced. A Robin-Robin domain decomposition algorithm applied on the interface boundary is introduced in Section 3 and its convergence behavior is analyzed. Numerical simulations are included in Section 4. In Section 5 some conclusions are presented.

2 Description of the model

Let us consider a two dimensional domain obtained as a section of a three dimensional realistic geometry. Assuming the symmetry of the geometry, we consider only a part of the section. Let $S \subset \mathbb{R}^2$ be a two dimensional domain which represents the polymeric part of the stent and $V \subset \mathbb{R}^2$ which represents the arterial wall. A schematic representation of the two dimensional domain used in this model is shown in Figure 1.

After implantation of the DES in the region of interest, the coated stent will be progressively covered by neointima. In this study we assume that the evolution of the vessel wall around the stent occurs instantaneously: this means in a very short period of time when compared with the period of drug release ([11, 19]). This is a simplification with respect to the complex dynamics of tissue healing and regrowth that takes place after stent implantation.

The following assumptions are taken into consideration in the mathematical model:

- The geometrical and mechanical effects of the stent strut (the metallic part of the stent) on the degradation of PLA are considered negligible;

- Viscoelastic properties of the polymeric part of the stent are considered negligible;

- The arterial wall is represented as an homogeneous viscoelastic porous media with the main properties of *Media*;

- Permeability and viscosity of the arterial wall are considered constants.

A mass transport process and a series of chemical reactions, which are responsible for the release of the drug and the degradation of the polymer, have been considered in the model.

2.1 Chemical reactions

We introduce in what follows the following notations:

$$\mathcal{M}_S = \left\{ W, P, O, L, SD, DD \right\}, \ \mathcal{M}_V = \left\{ W, O, L, DD \right\}, \tag{1}$$

where W, P, O, L, SD and DD respectively stand for fluid, PLA, oligomers, lactic acid, solid and dissolved drugs in the stent and

$$\mathcal{C}_S = \left(C_{m,S} \right)_{m \in \mathcal{M}_S}, \ \mathcal{C}_V = \left(C_{m,V} \right)_{m \in \mathcal{M}_V}, \tag{2}$$

represent concentration of molecules in the stent and in the arterial wall respectively.

Porosity and degradation

When the stent is inserted in the arterial wall, it enters in contact with the plasma. The biodegradable polymer reacts with the fluid and its molecular weight decreases due to polymer degradation. The porosity of the polymer increases as a result of erosion. These two aspects are considered in

the model and their influence in the release process is analyzed.

The effective diffusivity in the polymer coating ([18]) is defined by

$$D_{m,eff} = \frac{(1 - \phi_S)D_{m,S} + \lambda_S \phi_S D_{m,V}}{1 - \phi_S + \lambda_S \phi_S}, \quad m \in \mathcal{M}_S, \ m \neq P, SD. \tag{3}$$

It incorporates the diffusion coefficient of molecules in the polymer, $D_{m,S}$, the diffusion coefficient of molecules in the liquid-filled pores, $D_{m,V}$, the porosity ϕ_S of PLA, and the drug partitioning coefficient, λ_S, between the liquid-filled pores and the solid PLA phase.

The porosity of the PLA can be described by the following formulation ([18])

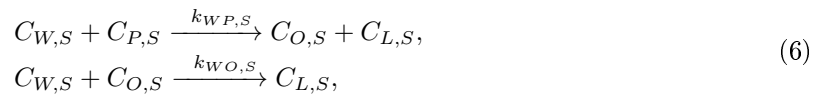$$\phi_S = \phi_{S,0} + (1 - \phi_{S,0})(1 + e^{-2k_{WP,S}t} - 2e^{-k_{WP,S}t}), \tag{4}$$

assuming the same density for PLA chains of different lengths. In (4), $\phi_{S,0}$ is the initial porosity in the PLA and the expression $1 + e^{-2k_{WP,S}t} - 2e^{-k_{WP,S}t}$, $t \geq 0$, represents erosion. It describes the mass loss as a function of time, where k_{WP} stands for a degradation rate constant. It is obvious that at $t = 0$, no erosion has occurred which means that the polymer is totally intact with initial porosity $\phi_{S,0}$, while at the end of the process the PLA is completely eroded and replaced by fluid ($\phi_S \to 1$) ([18]). The constant porosity $\phi_V = 0.61$ is considered for the arterial wall, ([19]).

The diffusion coefficients of the different species, oligomers, lactic acid and drug, in the polymer vary during the degradation process. As the polymer degradation proceeds, diffusional paths are opened through the polymer matrix pores, allowing dissolved drug molecules to leave the device via a degradation-controlled release ([16]). Hence, the diffusion coefficients in the coated stent follow the formula ([7, 14])

$$D_{m,S} = D_{m,S}^0 e^{\theta_{m,S} \frac{C_{P,S}^0 - C_{P,S}}{C_{P,S}^0}} \quad \text{in } \bar{S} \times \mathbb{R}^+, \ m \in \mathcal{M}_S, \ m \neq P, SD, \tag{5}$$

where $D_{m,S}^0$, $m \in \mathcal{M}_S$, $m \neq P, SD$, is the diffusion coefficient of the respective species in the polymer, $C_{P,S}^0$ is the concentration of polymer at $t = 0$ and $\theta_{m,S}$, $m \in \mathcal{M}_S$, $m \neq P, SD$, are experimental constants. In this paper, we assume that the diffusion coefficients in the arterial wall, $D_{m,V}$, $m \in \mathcal{M}_V$, are constants.

Two main reactions are responsible for the degradation of PLA into smaller molecules. The first reaction is the hydrolysis of the PLA producing oligomers which have smaller molecular weights M_W, $2 \times 10^4 \ g/mol \leq M_W \leq 1.2 \times 10^5 \ g/mol$. It is assumed that all of these oligomers have similar diffusion coefficients when they diffuse through the coated stent. The second reaction is the hydrolysis of the oligomers producing lactic acid with molecular weight $M_W \leq 2 \times 10^4 \ g/mol$. The lactic acid generated by this reaction is assumed to have a catalytic effect on further degradation of the PLA. These reactions are schematically the following:

$$\begin{aligned} C_{W,S} + C_{P,S} &\xrightarrow{k_{WP,S}} C_{O,S} + C_{L,S}, \\ C_{W,S} + C_{O,S} &\xrightarrow{k_{WO,S}} C_{L,S}, \end{aligned} \tag{6}$$

where $C_{W,S}$, $C_{P,S}$, $C_{O,S}$ and $C_{L,S}$ are the concentration in the coating of the fluid, PLA, oligomer and lactic acid in the polymeric stent respectively. When oligomers enter the arterial wall, they

convert into lactic acid in the presence of plasma by the following relation:

$$C_{W,V} + C_{O,V} \xrightarrow{k_{OW,V}} C_{L,V}. \tag{7}$$

Parameters $k_{PW,S}$, $k_{OW,S}$ and $k_{OW,V}$ represent the reaction rates of (6) and (7).

Drug dissolution

When the fluid diffuses through the polymeric matrix, the solid drug starts to dissolve accordingly to its thermodynamics and to the kinetics of the process. The dissolved drug diffuses through the polymer matrix. The process is schematically modeled by the following relation:

$$C_{W,S} + C_{SD,S} \xrightarrow{k_{DD,S}} C_{DD,S}, \tag{8}$$

where $C_{SD,S}$ and $C_{DD,S}$ stand for the concentrations of the solid drug (SD) and the dissolved drug (DD) respectively and $k_{DD,S}$ is the dissolution coefficient.

2.2 Convection in the arterial wall

The filtration of the plasma inside the arterial wall is driven by a decreasing pressure gradient from the inner layer of the artery (Γ_{lumen}) to the outer layer of the artery (Γ_{adv}). By consequence, we require that $p_V = p_{\text{lumen}}$ on Γ_{lumen} and $p_V = p_{\text{adv.}}$ on $\Gamma_{\text{adv.}}$ ([19]). As the dimensions of the stent are very small compared to the dimensions of the arterial wall, it is assumed that there is no convective transport in the stent.

Assuming that the arterial wall is a porous medium, the relation between the velocity field and the pressure drop is described by Darcy Law:

$$\begin{cases} u_V = -\frac{k_V}{\mu_V}\nabla p_V & \text{in } V, \\ \nabla . u_V = 0 & \text{in } V, \\ p_V = p_{lumen} & \text{on } \Gamma_{\text{lumen}}, \\ p_V = p_{adv} & \text{on } \Gamma_{\text{adv}}, \\ u_V . \eta_V = 0 & \text{on } \Gamma_{\text{wall}} \cup \Gamma_{\text{coat}}, \end{cases} \tag{9}$$

where u_V and p_V are the velocity field and the pressure in the arterial wall respectively. The coefficient k_V is the permeability of the medium, which characterizes the capacity of the arterial wall to allow permeation of small molecules. The permeability k_V, depends on the properties of the medium and also on the concentrations of oligomers, lactic acid and drug in the arterial wall. At the best of our knowledge a functional relation satisfied by k_V is not described in the literature. In this paper we assume that k_V is constant. In (9), μ_V is the viscosity of the fluid in the arterial wall which is the resistance of the fluid to flow. The viscosity μ_V depends on the chemical compounds present in the arterial wall. We assume in what follows that the viscosity μ_V is also constant ([6]).

2.3 The non-Fickian model

We couple now the phenomena taking place in the stent and in the vessel wall. The evolution of concentrations of molecules in (1) is described by the governing equations:

$$
\begin{cases}
\frac{\partial(\phi_S C_{m,S})}{\partial t} & = -\nabla.J(C_{m,S}) + F_{m,S}(\mathcal{C}_S) & \text{in } S \times \mathbb{R}^+, \ m \in \mathcal{M}_S, \ m \neq P, SD, \\
\frac{\partial C_{P,S}}{\partial t} & = F_{P,S}(\mathcal{C}_S) & \text{in } S \times \mathbb{R}^+, \\
\frac{\partial C_{SD,S}}{\partial t} & = F_{SD,S}(\mathcal{C}_S) & \text{in } S \times \mathbb{R}^+, \\
\frac{\partial C_{m,V}}{\partial t} & = -\nabla.J(C_{m,V}) + F_{m,V}(\mathcal{C}_V) & \text{in } V \times \mathbb{R}^+, \ m \in \mathcal{M}_V,
\end{cases}
\tag{10}
$$

where

$$
F_{m,S}(\mathcal{C}_S) =
\begin{cases}
-\sum\limits_{i=1,2} \mathcal{F}_{i,S}(\mathcal{C}_S), & \text{m=W}, \\
-\mathcal{F}_{1,S}(\mathcal{C}_S), & \text{m=P}, \\
\sum\limits_{i=1,2}(-1)^{i-1}\mathcal{F}_{i,S}(\mathcal{C}_S), & \text{m=O}, \\
\sum\limits_{i=1,2} \mathcal{F}_{i,S}(\mathcal{C}_S), & \text{m=L}, \\
\mathcal{F}_{3,S}(\mathcal{C}_S), & \text{m=DD}, \\
-\mathcal{F}_{3,S}(\mathcal{C}_S), & \text{m=SD},
\end{cases}
\tag{11}
$$

and

$$
F_{m,V}(\mathcal{C}_V) =
\begin{cases}
-\mathcal{F}_{1,V}(\mathcal{C}_V), & \text{m=W}, \\
\mathcal{F}_{1,V}(\mathcal{C}_V), & \text{m=O}, \\
\mathcal{F}_{1,V}(\mathcal{C}_V), & \text{m=L},
\end{cases}
\tag{12}
$$

and

$$
\begin{cases}
\mathcal{F}_{1,S}(\mathcal{C}_S) = k_{PW,S} C_{W,S} C_{P,S}\big(1 + \alpha C_{L,S}\big), \\
\mathcal{F}_{2,S}(\mathcal{C}_S) = k_{OW,S} C_{W,S} C_{O,S}\big(1 + \beta C_{L,S}\big), \\
\mathcal{F}_{3,S}(\mathcal{C}_S) = k_{DD,S} C_{W,S} C_{SD,S}, \\
\mathcal{F}_{1,V}(\mathcal{C}_V) = k_{OW,V} C_{W,V} C_{O,V}\big(1 + \gamma C_{L,V}\big).
\end{cases}
\tag{13}
$$

The mass fluxes in the stent and in the arterial wall in (10) are defined respectively by

$$
\begin{aligned}
J(C_{m,S}) &= -D_{m,eff}\nabla C_{m,S}, & m \in \mathcal{M}_S, \ m \neq P, SD, \\
J(C_{m,V}) &= -\Big(D_{m,V}\nabla C_{m,V} - u_V C_{m,V} + D_{m,\sigma_V}\sum_{i=1}^{n}\frac{\kappa_i}{\tau_i}\int_0^t e^{-\frac{t-s}{\tau_i}}\nabla C_{m,V}(s)ds\Big), & m \in \mathcal{M}_V.
\end{aligned}
\tag{14}
$$

The flux in the arterial wall is non Fickian ([6]). The integral term is a representation of $\nabla\sigma_V$, where σ_V represents the stress response of the arterial wall to the strain of the incoming molecules as given by Maxwell generalized model ([3]). In (14) $\tau_i = \frac{\eta_i}{\kappa_i}$, where the constants κ_i, $i = 1, \ldots, n$, represent the Young's modulus of the Maxwell arms while η_i, $i = 1, \ldots, n$, are their viscosities. The constants $D_{m,V}$ and D_{m,σ_V} are defined by

$$
\begin{aligned}
D_{m,V} &= \bar{D}_{m,V} + \alpha_{m,V}\big(\kappa_{r,V} + \sum_{i=1}^{n}\kappa_{i,V}\big)\bar{D}_{\sigma_V}, \\
D_{m,\sigma_V} &= k_{m,V}\bar{D}_{\sigma_V},
\end{aligned}
\tag{15}
$$

where $\bar{D}_{m,V}$ and $\bar{D}_{\sigma_V}$ are the diffusion and stress driven non-Fickian coefficients in the arterial wall respectively ([5, 6]). The multiple relaxation times used in this model are well adapted to predict the viscoelastic behavior in living tissues ([12]). For the rest of the paper, specific attention is devoted to the *Maxwell-Wiechert* viscoelastic model with $n = 1$.

In what follows we denote by $v(t)$ a function that depends on x, y and t, that is for each t, $v(t) : \bar{\Omega} \longrightarrow \mathbb{R}$, where $\bar{\Omega}$ represents $\bar{S}$ or $\bar{V}$.

To complete the coupled problem (10), we define the initial, the boundary and the interface conditions. At the initial time, we assume that the PLA and the solid drug are distributed uniformly in the stent. We also assume that at the initial time no degradation has occurred and consequently neither oligomers nor lactic acid are present in the coating. The initial concentrations in the coating and in the arterial wall are then given by

$$
\begin{cases}
C_{m,S}(0) = 0, & m \in \mathcal{M}_S, \ m \neq P, SD, \ C_{m,S}(0) = C_{m,S}^0, \ m = P, SD, \\
C_{W,V}(0) = C_{W,V}^0, \ C_{m,V}(0) = 0, & m \in \mathcal{M}_V, \ m \neq W.
\end{cases}
\tag{16}
$$

The boundary and interface conditions are summarized as follows:

$$
\begin{cases}
(\phi_S \lambda_S)^{-1} C_{m,S} = (\phi_V \lambda_V)^{-1} C_{m,V} & \text{on } \Gamma_{\text{coat}} \times \mathbb{R}^+, \ m \in \mathcal{M}_V, \\
J(C_{m,S}).\eta_S = -J(C_{m,V}).\eta_V & \text{on } \Gamma_{\text{coat}} \times \mathbb{R}^+, \ m \in \mathcal{M}_V, \\
J(C_{W,V}).\eta_V = \gamma_{W,V}(C_{W,out} - C_{W,V}) & \text{on } \Gamma_{\text{lumen}} \times \mathbb{R}^+, \\
J(C_{m,V}).\eta_V = -\gamma_{m,V} C_{m,V} & \text{on } \Gamma_{\text{lumen}} \times \mathbb{R}^+, \ m \in \mathcal{M}_V, m \neq W, \\
J(C_{m,V}).\eta_V = 0 & \text{on } (\Gamma_{\text{wall}} \cup \Gamma_{\text{adv}}) \times \mathbb{R}^+, \ m \in \mathcal{M}_V.
\end{cases}
\tag{17}
$$

As PLA has a large molecular weight ($M_W \geq 1.2 \times 10^5 g/mol$) compared to the other molecules present in the process, it does not diffuse and consequently no boundary condition is needed for the concentration of PLA.

The condition $(17)_1$ stands for the discontinuity of the diffusible molecules on the interface boundary Γ_{coat} where ϕ_j and λ_j, $j = S, V$, are the porosities and partitioning coefficients of the domains respectively. The condition $(17)_2$ stands for continuity of fluxes on the interface.

As the plasma penetrates from the blood artery into the arterial wall, we consider a natural boundary condition $(17)_3$ for the plasma where $C_{W,out}$ stands for the fluid concentration in the lumen. As the other molecules present in the arterial wall go directly to the blood and are transported very fast away from the region of interest, condition $(17)_4$ in considered for the lumen boundary Γ_{lumen}, with an high transference rate $\gamma_{m,V}$.

Symmetry on Γ_{wall} implies a non-flux condition $(17)_5$. As adventitia is considered impermeable to all species present in the arterial wall, the condition $(17)_5$ also holds for Γ_{adv}.

3   Robin-Robin domain decomposition method

In this section, we analyze a Robin-Robin domain decomposition algorithm to couple the polymeric stent to the arterial wall through the interface boundary Γ_{coat}.

3.1 Robin-Robin domain decomposition algorithm

We denote by $L^2(j)$ and $H^1(j)$, $j = S, V$, the usual Sobolev spaces endowed with the usual inner products $(.,.)_{L^2}$ and $(.,.)_{H^1}$ and norms $\|.\|_{L^2(j)}$ and $\|.\|_{H^1(j)}$, $j = S, V$, respectively ([1]).

Let $S_h = \bigcup\limits_{\Delta_S \in \mathcal{T}_{h_S}} \Delta_S$, $V_h = \bigcup\limits_{\Delta_V \in \mathcal{T}_{h_V}} \Delta_V$, where Δ_j, $j = S, V$, are the typical element of $\mathcal{T}_{h_j}$, the corresponding admissible discretization in $j = S, V$, respectively (Figure 2).

We introduce in $[0, T]$ a uniform grid $\left\{ t_n ; n = 0, \ldots, N \right\}$ with $t_0 = 0$, $t_N = T$, and $t_n - t_{n-1} = \Delta t$.

In what follows the approximation of a quantity will be identified by a subscript h and two superscripts n and k: the first identifies the time instant and the second one stands for the iteration. Consider

$$
\begin{aligned}
J(C_{m,S,h}^{n+1,k+1}) &= -D_{m,S} \nabla C_{m,S,h}^{n+1,k+1}, \ m \in \mathcal{M}_S, \ m \neq P, SD, \\
J(C_{m,V,h}^{n+1,k+1}) &= -\left(D_{m,V} \nabla C_{m,V,h}^{n+1,k+1} - u_{V,h} C_{m,V,h}^{n+1,k+1} + D_{m,\sigma_V} \sum_{i=0}^{n} e^{-\frac{(n-i)\Delta t}{\tau_V}} \nabla C_{m,V,h}^{n+1,k+1}(i\Delta t)\Delta t \right), \ m \in \mathcal{M}_V,
\end{aligned}
\tag{18}
$$

where $u_{V,h}$ is computed using the variational formulation for the Darcy's law (9) and for the sake of simplicity the diffusion coefficients $D_{m,j}$, $j = S, V$, and the porosities ϕ_j, $j = S, V$, are considered constants.

Considering

$$
\begin{aligned}
\mathcal{W}_h = \Bigg\{ \bigg((v_{m,S,h})_{\mathcal{M}_S}, (v_{m,V,h})_{\mathcal{M}_V} \bigg) \ &\in \big(C^0(\bar{S}_h) \big)^6 \times \big(C^0(\bar{V}_h) \big)^4 \\
&\text{such that } (\phi_{S,h}\lambda_S)^{-1} v_{m,S,h} = (\phi_{V,h}\lambda_V)^{-1} v_{m,V,h} \text{ on } \Gamma_{\text{coat},h}, \\
&\text{for } m \in \mathcal{M}_V, \ \bigg((v_{m,S,h})_{\mathcal{M}_S}, (v_{m,V,h})_{\mathcal{M}_V} \bigg) \Big|_{\Delta_S \times \Delta_V} \in (P_r)^6 \times (P_r)^4, \\
&\Delta_S \in \mathcal{T}_{h_S}, \Delta_V \in \mathcal{T}_{h_V} \Bigg\},
\end{aligned}
\tag{19}
$$

where P_r denotes the space of polynomials of degree at most r, we have the following variational formulations:

Find $\bigg((C_{m,S,h}^{n+1,k+1})_{\mathcal{M}_S}, (C_{m,V,h}^{n+1,k+1})_{\mathcal{M}_V} \bigg) \in \mathcal{W}_h$ such that

$$
\begin{cases}
\displaystyle\sum_{j=S,V} \sum_{m\in\mathcal{M}_j} \left(\frac{C_{m,j,h}^{n+1,k+1} - C_{m,j,h}^{n,k+1}}{\Delta t}, v_{m,j,h} \right)_{j_h} = \sum_{\substack{m\in\mathcal{M}_S \\ m\neq P,SD}} \left(J(C_{m,S,h}^{n+1,k+1}), \nabla v_{m,S,h} \right)_{S_h} + \sum_{m\in\mathcal{M}_V} \left(J(C_{m,V,h}^{n+1,k+1}), \nabla v_{m,V,h} \right)_{V_h} \\
\qquad\qquad + \displaystyle\sum_{j=S,V} \sum_{m\in\mathcal{M}_j} \left(F_{m,j,h}^{n+1,k+1}(\mathcal{C}_{j,h}), v_{m,j,h} \right)_{j_h} \\
\qquad\qquad + \gamma_{W,V} \left(C_{W,out} - C_{W,V,h}^{n+1,k+1}, v_{W,V,h} \right)_{\Gamma_{\text{lumen},h}} \\
\qquad\qquad - \displaystyle\sum_{\substack{m\in\mathcal{M}_V \\ m\neq W}} \gamma_{m,V} \left(C_{m,V,h}^{n+1,k+1}, v_{m,V,h} \right)_{\Gamma_{\text{lumen},h}}, \\
\text{for all } \bigg((v_{m,S,h})_{\mathcal{M}_S}, (v_{m,V,h})_{\mathcal{M}_V} \bigg) \in \mathcal{W}_h, \\
\mathcal{C}_{S,h}^{0,1} = (0,1,0,0,0,1), \mathcal{C}_{V,h}^{0,1} = (1,0,0,0),
\end{cases}
\tag{20}
$$

To establish the Robin-Robin interface boundary condition on $\Gamma_{\text{coat},h}$, we consider the following algorithm:

Algorithm 1 *Robin-Robin* Iterative Scheme

$C_{m,S,h}^{0,1}, \ D_{m,S}, \ m \in \mathcal{M}_S, \ C_{m,V,h}^{0,1}, \ D_{m,\sigma}, \ D_{m,V}, \ m \in \mathcal{M}_V$, and $\tau_1, \gamma_{1,V}$ and $\varepsilon > 0$ are given.

Take n and Δt such that $N = n\Delta t$, $\left((v_{m,S,h})_{\mathcal{M}_S}, (v_{m,V,h})_{\mathcal{M}_V} \right) \subset \mathcal{W}_h$.

For $n = 0, \ldots, N$,
For $k \geq 0$,
Solve

$$\begin{cases} \displaystyle\sum_{m \in \mathcal{M}_S} \left(\frac{C_{m,S,h}^{n+1,k+1} - C_{m,S,h}^{n,k+1}}{\Delta t}, v_{m,S,h} \right)_{S_h} = \displaystyle\sum_{\substack{m \in \mathcal{M}_S \\ m \neq P, SD}} \left(J(C_{m,S,h}^{n+1,k+1}), \nabla v_{m,S,h} \right)_{S_h} \\ \qquad\qquad\qquad\qquad\qquad\qquad\qquad + \displaystyle\sum_{m \in \mathcal{M}_S} \left(F_{m,S,h}^{n+1,k+1}(\mathcal{C}_{S,h}), v_{m,S,h} \right)_{S_h}, \quad \text{in } S_h, \\[4mm] \displaystyle\sum_{m \in \mathcal{M}_V} (J(C_{m,S,h}^{n+1,k+1}).\eta_S + \delta_S C_{m,S,h}^{n+1,k+1}, v_{m,S,h})_{\Gamma_{\text{coat}},h} = - \displaystyle\sum_{m \in \mathcal{M}_V} (J(C_{m,V,h}^{n+1,k}).\eta_V - \delta_V C_{m,V,h}^{n+1,k}, v_{m,V,h})_{\Gamma_{\text{coat}},h}. \end{cases} \quad (21)$$

Solve

$$\begin{cases} \displaystyle\sum_{m \in \mathcal{M}_V} \left(\frac{C_{m,V,h}^{n+1,k+1} - C_{m,V,h}^{n,k+1}}{\Delta t}, v_{m,V,h} \right)_{V_h} = \displaystyle\sum_{m \in \mathcal{M}_V} \left(J(C_{m,V,h}^{n+1,k+1}), \nabla v_{m,V,h} \right)_{V_h} \\ \qquad\qquad\qquad\qquad\qquad\qquad + \displaystyle\sum_{m \in \mathcal{M}_V} \left(F_{m,V,h}^{n+1,k+1}(\mathcal{C}_{V,h}), v_{m,V,h} \right)_{V_h} \\ \qquad\qquad\qquad\qquad\qquad\qquad + \gamma_{W,V} \left(C_{W,out} - C_{W,V,h}^{n+1,k+1}, v_{W,V,h} \right)_{\Gamma_{\text{lumen}},h} \quad \text{in } V_h, \\ \qquad\qquad\qquad\qquad\qquad\qquad - \displaystyle\sum_{\substack{m \in \mathcal{M}_V \\ m \neq W}} \gamma_{m,V} \left(C_{m,V,h}^{n+1,k+1}, v_{m,V,h} \right)_{\Gamma_{\text{lumen}},h}, \\[4mm] \displaystyle\sum_{m \in \mathcal{M}_V} (J(C_{m,V,h}^{n+1,k+1}).\eta_V - \delta_V C_{m,V,h}^{n+1,k+1}, v_{m,V,h})_{\Gamma_{\text{coat}},h} = - \displaystyle\sum_{m \in \mathcal{M}_V} (J(C_{m,S,h}^{n+1,k+1}).\eta_S + \delta_S C_{m,S,h}^{n+1,k+1}, v_{m,S,h})_{\Gamma_{\text{coat}},h}. \end{cases} \quad (22)$$

If $\displaystyle\max_{m \in \mathcal{M}_V} \left\| \delta_V C_{m,V,h}^{n+1,k+1} - \delta_S C_{m,S,h}^{n+1,k+1} \right\|_{L_\infty(\Gamma_{\text{coat}},h)} \leq \varepsilon$ then stop,
Else k:=k+1,
End (for k),
n:=n+1,
End (for n).

where $\delta_j = \frac{1}{\lambda_j \phi_j} > 0, \ j = S, V$, are non-negative acceleration parameters responsible for porosities and partitioning coefficients of domains.

3.2 Stability of Robin-Robin iterative method

In this section, we study the stability of the Robin-Robin iterative method, introduced in the previous section, in the simplified situation $\delta_S = \delta_V = \delta$.
Consider $\mathcal{W}_{m,j,h}^{n,k} = C_{m,j,h}^{n,k} - \tilde{C}_{m,j,h}^{n,k}, \ j = S, V$, where $C_{m,j,h}^{n,k}$ and $\tilde{C}_{m,j,h}^{n,k}$ are two different finite element solutions of the system (10) at time level n and iteration k.
We first linearize the term $F_{m,V,h}^{n+1,k+1}(C_{m,V,h}^{n+1,k+1}) - F_{m,V,h}^{n+1,k+1}(\tilde{C}_{m,V,h}^{n+1,k+1}), \ m \in \mathcal{M}_V$, around the solution $C_{m,V,h}^{n+1,k+1}$. We get

$$F_{m,V,h}^{n+1,k+1}(C_{m,V,h}^{n+1,k+1}) - F_{m,V,h}^{n+1,k+1}(\tilde{C}_{m,V,h}^{n+1,k+1}) \simeq \mathbb{F}_J(C_{m,V,h}^{n+1,k+1})\mathcal{W}_{m,V,h}^{n+1,k+1} = \begin{cases} -\mathcal{F}_J(C_{m,V,h}^{n+1,k+1})\mathcal{W}_{m,V,h}^{n+1,k+1}, & \text{m=W}, \\ -\mathcal{F}_J(C_{m,V,h}^{n+1,k+1})\mathcal{W}_{m,V,h}^{n+1,k+1}, & \text{m=O}, \\ \mathcal{F}_J(C_{m,V,h}^{n+1,k+1})\mathcal{W}_{m,V,h}^{n+1,k+1}, & \text{m=L}, \end{cases} \quad (23)$$

where $\mathcal{F}_J(C_{m,V,h}^{n+1,k+1})\mathcal{W}_{m,V,h}^{n+1,k+1}$, represents the Fréchet derivative ([8]) given by

$$
\begin{aligned}
\mathcal{F}_J(C_{m,V,h}^{n+1,k+1})\mathcal{W}_{m,V,h}^{n+1,k+1} &= \kappa_{OW,V}C_{O,V,h}^{n+1,k+1}(1+\gamma C_{L,V,h}^{n+1,k+1})\mathcal{W}_{W,V,h}^{n+1,k+1} \\
&+\kappa_{OW,V}C_{W,V,h}^{n+1,k+1}(1+\gamma C_{L,V,h}^{n+1,k+1})\mathcal{W}_{O,V,h}^{n+1,k+1} \\
&+\kappa_{OW,V}\gamma C_{W,V,h}^{n+1,k+1}C_{O,V,h}^{n+1,k+1}\mathcal{W}_{L,V,h}^{n+1,k+1}.
\end{aligned}
\tag{24}
$$

There is a positive constant $\mathcal{K}_{V,h}$ depends on $\left\|C_{V,h}^*\right\|_{L^\infty} = \max_{m\in\mathcal{M}_V}\left\|C_{m,V,h}^{n+1,k+1}\right\|_{L^\infty}$ such that

$$
\sum_{m\in\mathcal{M}_V}\int_{V_h}\mathbb{F}_J(C_{m,V,h}^{n+1,k+1})\mathcal{W}_{m,V,h}^{n+1,k+1}\mathcal{W}_{m,V,h}^{n+1,k+1}ds \leq \mathcal{K}_{V,h}\sum_{m\in\mathcal{M}_V}\left\|\mathcal{W}_{m,V,h}^{n+1,k+1}\right\|_{V_h}^2.
\tag{25}
$$

By re-writing (22) for $\mathcal{W}_{m,V,h}^{n+1,k+1}$, taking $v_{m,V,h}=\mathcal{W}_{m,V,h}^{n+1,k+1}$ in (22) and taking (25) into consideration, we obtain

$$
\begin{aligned}
\sum_{m\in\mathcal{M}_V}\left\|\mathcal{W}_{m,V,h}^{n+1,k+1}\right\|_{V_h}^2 &+2\Delta t\sum_{m\in\mathcal{M}_V}\int_{\Gamma_{\text{coat}}}J(\mathcal{W}_{m,V,h}^{n+1,k+1})\mathcal{W}_{m,V,h}^{n+1,k+1}ds \\
&-2\Delta t\mathcal{K}_{V,h}\sum_{m\in\mathcal{M}_V}\left\|\mathcal{W}_{m,V,h}^{n+1,k+1}\right\|_{V_h}^2 dV \\
&\leq 2\Delta t\sum_{m\in\mathcal{M}_V}\int_{V_h}J(\mathcal{W}_{m,V,h}^{n+1,k+1})\nabla\mathcal{W}_{m,V,h}^{n+1,k+1}dV + \sum_{m\in\mathcal{M}_V}\left\|\mathcal{W}_{m,V,h}^{n,k+1}\right\|_{V_h}^2.
\end{aligned}
\tag{26}
$$

Using the Cauchy inequality with $\epsilon_m > 0$, $m\in\mathcal{M}_V$ ([4]), the inequality

$$
\left(u_{V,h}\mathcal{W}_{m,V,h}^{n+1,k+1}, \nabla\mathcal{W}_{m,V,h}^{n+1,k+1}\right)_{V_h} \leq \frac{\|u_{V,h}\|_\infty}{2}\left(\left\|\mathcal{W}_{m,V,h}^{n+1,k+1}\right\|_{L^2(V_h)}^2 + \left\|\nabla\mathcal{W}_{m,V,h}^{n+1,k+1}\right\|_{L^2(V_h)}^2\right),
\tag{27}
$$

holds for $m\in\mathcal{M}_V$.

Considering the inequality

$$
\begin{aligned}
-\int_{V_h}&\left(\sum_{i=0}^n e^{-\frac{(n-i)\Delta t}{\tau_1}}\mathcal{W}_{m,V,h}^{n+1,k+1}(i\Delta t)\Delta t\right)\mathcal{W}_{m,V,h}^{n+1,k+1}(n\Delta t)dV \\
&= -\frac{1}{2\Delta t}\left(\left\|\sum_{i=0}^n e^{-\frac{(n-i)\Delta t}{\tau_1}}\mathcal{W}_{m,V,h}^{n+1,k+1}(i\Delta t)\Delta t - \sum_{i=0}^n e^{-\frac{(n-i)\Delta t}{\tau_1}}\mathcal{W}_{m,V,h}^{n,k+1}(i\Delta t)\Delta t\right\|_{V_h}^2\right) \\
&\quad -\frac{1}{\tau_1}\left\|\sum_{i=0}^n e^{-\frac{(n-i)\Delta t}{\tau_1}}\mathcal{W}_{m,V,h}^{n+1,k+1}(i\Delta t)\Delta t\right\|_{V_h}^2 \\
&\leq -\frac{1}{2\Delta t}\left(\left\|\sum_{i=0}^n e^{-\frac{(n-i)\Delta t}{\tau_1}}\mathcal{W}_{m,V,h}^{n+1,k+1}(i\Delta t)\Delta t\right\|_{V_h}^2 - \left\|\sum_{i=0}^n e^{-\frac{(n-i)\Delta t}{\tau_1}}\mathcal{W}_{m,V,h}^{n,k+1}(i\Delta t)\Delta t\right\|_{V_h}^2\right) \\
&\quad -\frac{1}{\tau_1}\left\|\sum_{i=0}^n e^{-\frac{(n-i)\Delta t}{\tau_1}}\mathcal{W}_{m,V,h}^{n+1,k+1}(i\Delta t)\Delta t\right\|_{V_h}^2 \\
&\leq -\left(\frac{1}{2}+\frac{\Delta t}{\tau_1}\right)\left\|\sum_{i=0}^n e^{-\frac{(n-i)\Delta t}{\tau_1}}\mathcal{W}_{m,V,h}^{n+1,k+1}(i\Delta t)\right\|_{V_h}^2 + \frac{1}{2}\left\|\sum_{i=0}^n e^{-\frac{(n-i)\Delta t}{\tau_1}}\mathcal{W}_{m,V,h}^{n,k+1}(i\Delta t)\right\|_{V_h}^2.
\end{aligned}
\tag{28}
$$

and taking (27) into consideration, we obtain

$$
\begin{aligned}
&\int_{V_h} J(\mathcal{W}_{m,V,h}^{n+1,k+1}) \nabla \mathcal{W}_{m,V,h}^{n+1,k+1} dV \\
&= -\int_{V_h} \left(D_{m,V} \nabla \mathcal{W}_{m,V,h}^{n+1,k+1} - u_{V,h} \mathcal{W}_{m,V,h}^{n+1,k+1} + D_{m,\sigma_V} \sum_{i=0}^{n} e^{-\frac{(n-i)\Delta t}{\tau_V}} \nabla \mathcal{W}_{m,V,h}^{n+1,k+1}(i\Delta t)\Delta t \right) \nabla \mathcal{W}_{m,V,h}^{n+1,k+1} dV \\
&\leq -\left(D_{m,V} - \frac{\|u_{V,h}\|_\infty}{2} \right) \left\| \nabla \mathcal{W}_{m,V,h}^{n+1,k+1} \right\|_{V_h}^2 + \frac{\|u_{V,h}\|_\infty}{2} \left\| \mathcal{W}_{m,V,h}^{n+1,k+1} \right\|_{V_h}^2 \\
&\quad -D_{m,\sigma_V}\left(\frac{1}{2} + \frac{\Delta t}{\tau_1}\right) \left\| \sum_{i=0}^{n} e^{-\frac{(n-i)\Delta t}{\tau_1}} \mathcal{W}_{m,V,h}^{n+1,k+1}(i\Delta t) \right\|_{V_h}^2 + \frac{D_{m,\sigma_V}}{2} \left\| \sum_{i=0}^{n} e^{-\frac{(n-i)\Delta t}{\tau_1}} \mathcal{W}_{m,V,h}^{n,k+1}(i\Delta t) \right\|_{V_h}^2,
\end{aligned}
\tag{29}
$$

for $m \in \mathcal{M}_V$.

Using the identity

$$
\left(A + \delta B \right)^2 - \left(A - \delta B \right)^2 - 4\delta AB = 0,
\tag{30}
$$

we have

$$
\begin{aligned}
\int_{\Gamma_{\mathrm{coat}}} \left(J(\mathcal{W}_{m,V,h}^{n+1,k+1}).\eta_V \right) \mathcal{W}_{m,V,h}^{k+1,k+1} ds &= \frac{1}{4\delta} \int_{\Gamma_{\mathrm{coat}}} \left(J(\mathcal{W}_{m,V,h}^{n+1,k+1}).\eta_V - \delta \mathcal{W}_{m,V,h}^{n+1,k+1} \right)^2 ds \\
&\quad - \frac{1}{4\delta} \int_{\Gamma_{\mathrm{coat}}} \left(J(\mathcal{W}_{m,V,h}^{n+1,k+1}).\eta_V + \delta \mathcal{W}_{m,V,h}^{n+1,k+1} \right)^2 ds.
\end{aligned}
\tag{31}
$$

Using the interface condition $(21)_2$, we will have

$$
\begin{aligned}
\int_{\Gamma_{\mathrm{coat}}} \left(J(\mathcal{W}_{m,V,h}^{n+1,k+1}).\eta_V \right) \mathcal{W}_{m,V,h}^{n+1,k+1} ds &+ \frac{1}{4\delta} \int_{\Gamma_{\mathrm{coat}}} \left(-J(\mathcal{W}_{m,V,h}^{n+1,k+1}).\eta_V + \delta \mathcal{W}_{m,V,h}^{n+1,k+1} \right)^2 ds \\
&= \frac{1}{4\delta} \int_{\Gamma_{\mathrm{coat}}} \left(J(\mathcal{W}_{m,S,h}^{n+1,k+1}).\eta_S - \delta \mathcal{W}_{m,S,h}^{n+1,k+1} \right)^2 ds.
\end{aligned}
\tag{32}
$$

Using the same argument (as in equation (31)) for $\mathcal{W}_{m,S,h}^{n+1,k+1}$, $m \in \mathcal{M}_V$ and the interface condition $(22)_2$, we have

$$
\begin{aligned}
\int_{\Gamma_{\mathrm{coat}}} \left(J(\mathcal{W}_{m,S,h}^{n+1,k+1}).\eta_S \right) \mathcal{W}_{m,S,h}^{n+1,k+1} ds &+ \frac{1}{4\delta} \int_{\Gamma_{\mathrm{coat}}} \left(J(\mathcal{W}_{m,S,h}^{n+1,k+1}).\eta_S - \delta \mathcal{W}_{m,S,h}^{n+1,k+1} \right)^2 ds \\
&= -\frac{1}{4\delta} \int_{\Gamma_{\mathrm{coat}}} \left(J(\mathcal{W}_{m,V,h}^{n+1,k}).\eta_V - \delta \mathcal{W}_{m,V,h}^{n+1,k} \right)^2 ds.
\end{aligned}
\tag{33}
$$

Adding (32) and (33) and then summing up from $k = 0$ to $k = M$, we obtain

$$
\begin{aligned}
\sum_{k=0}^{M} \sum_{m \in \mathcal{M}_V} &\left(\int_{\Gamma_{\mathrm{coat}}} \left(J(\mathcal{W}_{m,V,h}^{n+1,k+1}).\eta_V \right) \mathcal{W}_{m,V,h}^{n+1,k+1} ds + \int_{\Gamma_{\mathrm{coat}}} \left(J(\mathcal{W}_{m,S,h}^{n+1,k+1}).\eta_S \right) \mathcal{W}_{m,S,h}^{n+1,k+1} ds \right) \\
&= \frac{1}{4\delta} \sum_{m \in \mathcal{M}_V} \left(\int_{\Gamma_{\mathrm{coat}}} \left(-J(\mathcal{W}_{m,V,h}^{n+1,0}).\eta_S + \delta \mathcal{W}_{m,V,h}^{n+1,0} \right)^2 ds - \int_{\Gamma_{\mathrm{coat}}} \left(-J(\mathcal{W}_{m,V,h}^{n+1,M+1}).\eta_V + \delta \mathcal{W}_{m,V,h}^{n+1,M+1} \right)^2 ds \right).
\end{aligned}
\tag{34}
$$

The series

$$
\sum_{k=0}^{\infty} \sum_{m \in \mathcal{M}_V} \left(\int_{\Gamma_{\mathrm{coat}}} \left(J(\mathcal{W}_{m,V,h}^{n+1,k+1}).\eta_V \right) \mathcal{W}_{m,V,h}^{n+1,k+1} ds + \int_{\Gamma_{\mathrm{coat}}} \left(J(\mathcal{W}_{m,S,h}^{n+1,k+1}).\eta_S \right) \mathcal{W}_{m,S,h}^{n+1,k+1} ds \right),
\tag{35}
$$

11

is convergent as in (34), $\sum_{k=0}^{M} f(k) + g(M) = \text{const}$, where

$$f(k) = \sum_{m \in \mathcal{M}_V} \left(\int_{\Gamma_{\text{coat}}} \left(J(\mathcal{W}_{m,V,h}^{n+1,k+1}).\eta_V \right) \mathcal{W}_{m,V,h}^{n+1,k+1} ds + \int_{\Gamma_{\text{coat}}} \left(J(\mathcal{W}_{m,S,h}^{n+1,k+1}).\eta_S \right) \mathcal{W}_{m,S,h}^{n+1,k+1} ds \right), \quad (36)$$

and

$$g(M) = \frac{1}{4\delta} \int_{\Gamma_{\text{coat}}} \left(-J(\mathcal{W}_{m,V,h}^{n+1,M+1}).\eta_V + \delta \mathcal{W}_{m,V,h}^{n+1,M+1} \right)^2 ds. \quad (37)$$

As $\sum_{k=0}^{M+1} f(k) + g(M+1) = \text{const}$, we easily deduce $g(M) = f(M+1) + g(M+1)$.
So we have

$$\sum_{k=0}^{M} f(k) + g(M+1) + f(M+1) = \text{const}. \quad (38)$$

Taking the limit in both side of (38), we get

$$\lim_{M \to \infty} \left(\sum_{k=0}^{M} f(k) + g(M+1) + f(M+1) \right) = \text{const}, \quad (39)$$

consequently

$$\lim_{M \to \infty} \left(\sum_{k=0}^{M} f(k) + g(M) + f(M+1) \right) = \text{const}, \quad (40)$$

and as $\lim_{m \to \infty} \left(\sum_{k=0}^{M} f(k) + g(M) \right) = \text{const}$, we conclude that $\lim_{m \to \infty} f(M+1) = 0$.
Using (26), the inequality

$$
\begin{aligned}
&\sum_{m \in \mathcal{M}_V} \left(\left(1 - 2\Delta t \left(\mathcal{K}_{V,h} + \frac{\|u_{V,h}\|_\infty}{2} \right) \right) \left\| \mathcal{W}_{m,V,h}^{n+1,k+1} \right\|_{V_h}^2 \right. \\
&+ 2\Delta t \left(D_{m,V} - \frac{\|u_{V,h}\|_\infty}{2} \right) \left\| \nabla \mathcal{W}_{m,V,h}^{n+1,k+1} \right\|_{V_h}^2 \\
&+ 2\Delta t D_{m,\sigma_V} \left(\frac{1}{2} + \frac{\Delta t}{\tau_1} \right) \left\| \sum_{i=0}^{n} e^{-\frac{(n-i)\Delta t}{\tau_1}} \mathcal{W}_{m,V,h}^{n+1,k+1}(i\Delta t) \right\|_{V_h}^2 \right) \\
&+ \sum_{m \in \mathcal{M}_S} \left(\left(1 - 2\Delta t \mathcal{K}_{S,h} \right) \left\| \mathcal{W}_{m,S,h}^{n+1,k+1} \right\|_{S_h}^2 + 2\Delta t D_{m,S} \left\| \nabla \mathcal{W}_{m,S,h}^{n+1,k+1} \right\|_{S_h}^2 \right) \\
&\leq \sum_{j=S,V} \sum_{m \in \mathcal{M}_j} \left\| \mathcal{W}_{m,j,h}^{n,k+1} \right\|_{j_h}^2 + \Delta t \sum_{m \in \mathcal{M}_V} D_{m,\sigma_V} \left\| \sum_{i=0}^{n} e^{-\frac{(n-i)\Delta t}{\tau_1}} \mathcal{W}_{m,V,h}^{n+1,k+1}(i\Delta t) \right\|_{V_h}^2,
\end{aligned}
\quad (41)
$$

holds and the energy functional

$$\mathcal{E}^{(n+1)} = \lim_{k \to \infty} \sum_{j=S,V} \sum_{m \in \mathcal{M}_j} \left(\left\| \mathcal{W}_{m,j,h}^{n+1,k+1} \right\|_{j_h}^2 + \left\| \nabla \mathcal{W}_{m,j,h}^{n+1,k+1} \right\|_{j_h}^2 \right) + \Delta t \sum_{m \in \mathcal{M}_V} \left\| \sum_{i=0}^{n} e^{-\frac{(n-i)\Delta t}{\tau_1}} \mathcal{W}_{m,V,h}^{n+1,k+1}(i\Delta t) \right\|_{V_h}^2, \quad (42)$$

satisfies in the inequality

$$\mathcal{E}^{(n+1)} \leq \theta\mathcal{E}^{(n)} \leq \theta^{n+1}\mathcal{E}^{(0)}, \tag{43}$$

such that

$$\theta = \frac{1}{\min\left(k_{V,1}, k_{V,2}, k_{V,3}, k_{S,1}, k_{S,2}\right)}, \tag{44}$$

and

$$
\begin{aligned}
k_{V,1} &= 1 - 2\Delta t\big(\mathcal{K}_{V,h} + \frac{\left\|u_{V,h}\right\|_\infty}{2}\big), \\
k_{V,2} &= \min_{m \in \mathcal{M}_V}\left\{2\big(D_{m,V} - \frac{\left\|u_{V,h}\right\|_\infty}{2}\big)\right\}, \\
k_{V,3} &= \min_{m \in \mathcal{M}_V}\left\{D_{m,\sigma_V}\big(1 + \frac{2\Delta t}{\tau_1}\big)\right\} \\
k_{S,1} &= 1 - 2\Delta t\mathcal{K}_{S,h}, \\
k_{S,2} &= \min_{m \in \mathcal{M}_S}\left\{2D_{m,S}\right\}.
\end{aligned}
\tag{45}
$$

The inequality (43) holds if

$$\Delta t < \min\left\{\frac{1}{2\mathcal{K}_{V,h} + \left\|u_{V,h}\right\|_\infty}, \frac{1}{2\mathcal{K}_{S,h}}\right\}, \ D_{m,V} > \frac{\left\|u_{V,h}\right\|_\infty}{2}, \ D_{m,\sigma_V} > 0, \ m \in \mathcal{M}_V \text{ and } D_{m,S} > 0, \ m \in \mathcal{M}_S. \tag{46}$$

The estimate (43) allows us to conclude the stability of the proposed method.

4   Numerical experiments

The governing equations are discretized in space with the finite element method using the commercial software package COMSOL Multiphysics 5.1 (COMSOL AB, Burlington, MA, USA.
To reduce the computational cost, we assume that the domain consists only of two PLA based strut and fully-embedded in a straight arterial wall. The coating and arterial wall domains are meshed as illustrated in Figure 2, where a finer mesh in the coating than the arterial wall is used, considering the much smaller scale of the coating domain. Refined meshes are also used at the stent-wall interfaces to improve the simulation accuracy. We have used *PDE interfaces, General Form PDE sub-module* in the *Mathematics module* to have more flexibility to define the system of equations in COMSOL.
The time integration is performed with a backward differential formula (BDF) with a time step size of 1 second, while the space is discretized by quadratic finite elements (P_2) with the average mesh size in the stent $29.8\mu m$ (323 elements) and in the arterial wall $56.7\mu m$ (1112 elements) respectively. The thickness of the media ($2 \times 10^{-2}cm$) and the stent ($5 \times 10^{-4}cm$) have been extracted from [19] and [13].
Parameters in Table 1 which have been extracted from [2,10,13,14] and [19], are used in all numerical experiments. The computational time for the reference simulation performed on an Intel(R) Core(TM) i7-4790 3.60 GHz processor, 16.0 GB RAM and 64-bit operating system is around 1

hour.

In Figure 3 the effect of the degradation rate on the porosity of the polymer is shown. We observe that a larger degradation rate increases the porosity of the polymer. This observation suggests that more fluid penetration and speed-up of the drug release will occur. We will illustrate this aspect in Figures 7 and 8.

Figure 4 shows the pressure distribution in the arterial wall while the arrows indicate the velocity field. The average pressure and velocity are 70.85 mmHg and $5.94 \times 10^{-6} \frac{m}{s}$ respectively.

The release of drug during the first month of the stent implantation is shown in Figure 5. Less drug concentration is observed in the lumen boundary as it is washed out by the blood flow.

Figure 6 shows the time evolution of the mass of the dissolved and solid drugs in the polymeric stent. We observe that the mass of the dissolved drug in the stent first increases but due to its release into the arterial wall, it then decreases.

In Figures 7 and 8, the effect of the polymer degradation rate on the accumulation of the dissolved drug in the stent and in the arterial wall are shown. It is observed that a larger polymeric degradation rate decreases the maximum amount of drug accumulations in both domains. In other words, with a smaller degradation rate, a higher initial burst of the dissolved drug in the stent and in the arterial wall could be expected.

In Figure 9 the effect of different diffusion coefficients on the amount of dissolved drug in the stent has been compared. In the case of effective diffusion coefficient (3), when the plasma penetrates the stent, it breaks the chemical chains of the polymer and increases polymer's erosion. This causes more fluid entrance into the stent and more degradation in the polymer. Consequently the dissolved drug leaves faster the stent than the case of a constant diffusion coefficient.

Figure 10 illustrates that changing the diffusion coefficients of molecules (specially fluid and dissolved drug) in the stent influences the amount of drug in the arterial wall. In the case of a biodegradable polymer, where the effective diffusion coefficients in the stent are given by (3), the drug accumulates more in the arterial wall before its peak. When a fixed diffusion coefficient is used, the drug has a larger residence time in the arterial wall than in the case a variable diffusion coefficient is used. This is due to the fact that in the case of effective diffusion coefficient, the dissolved drug leaves the stent faster and reaches the arterial wall quicker.

It is observed that in the case the effective diffusion coefficient is used for the plasma (3), more fluid enters the stent (see Figure 11) which causes more degradation and eventually more lactic acid and oligomers concentrations in the stent and in the arterial wall.

Figure 12 illustrates that in the case the effective diffusion coefficient (3) is used, more lactic acid is produced and accumulates in the arterial wall. One main concern with the use of PLA is that its degradation products reduce local pH, which can originate an inflammatory response. In this sense the amount of lactic acid is an important information because its accumulation in the smooth muscles surrounding arteries is a cause of plaques formation.

In Figures 13 and 14, the effect of the dissolution rate on the mass of the dissolved drug both in the stent and in the arterial wall are shown. It is observed that the larger dissolution rate leads to the largest peaks of drug in both domains. However a steepest decay of the mass is also observed leading to a shorter residence time.

Figure 14 illustrates that in the case of an initial burst, the drug leaves the arterial wall faster and it is washed out by the blood flow through Γ_{lumen}. As a result, to have a more sustainable drug

release, with a larger residence time in the arterial wall, a drug with a smaller dissolution rate should be used in the stent. The weak water solubility avoids rapid release into the circulation.

5 Conclusions

In recent years mathematical modeling has become an effective tool to simulate drug delivery processes. In the case of drug eluting stents it leads to a deeper understanding of the drug release mechanisms in the biodegradable coating and in the arterial wall. Although cardiovascular drug delivery depends on very complex biochemical and physiological phenomena, we believe that a simplified release model can help to provide understanding of the dependence of drug pharmacokinetics on the properties of the three main actors of the process. The three main actors that interact in the drug release are the coated stent, the drug, and the vessel wall. Concerning the device we mention the properties of the polymeric coating, as the degradation rate and its time dependent porosity. Regarding the vessel properties, we refer to the stiffness of the vessel walls and its influence on the the drug delivery profile. Finally as far as the drug properties are concerned we mention the importance of its dissolution rate. All these properties have been included in the model presented in this paper. The sensitivity of the process relatively to the parameters that characterize these properties are analyzed.

In a previous paper ([6]) by some of the authors, the influence of arterial stiffness on the drug release was studied. In this paper, while keeping in the model the stiffness of the vessel walls, a more realistic description of the polymeric coating, namely its time dependent porosity, is included. The coating of the stent is biodegradable and the influence of the time dependent porosity of PLA on the release of drug into the arterial wall has been analyzed. The numerical results suggest that drug leaves faster the polymer when the effect of time dependent porosity is considered. The results also show that in this case the residence time of the drug in the arterial wall is shorter. The numerical simulations also illustrate that to have a more sustained drug accumulation in the arterial wall, a drug with a smaller dissolution rate should be used.

Conflict of interest statement

The authors declare that no conflict of interest occurs.

Acknowledgements

References

[1] R. ADAMS AND J. FOURNIER, *Sobolev spaces*, Elsevier 2nd edition, 2003.

[2] F. BOZSAK, J.-M. CHOMAZ, AND A. I. BARAKAT, *Modeling the transport of drugs eluted from stents: physical phenomena driving drug distribution in the arterial wall.*, Biomechanics and modeling in mechanobiology, 13 (2014), pp. 327–47.

[3] H. F. BRINSON AND L. C. BRINSON, *Polymer Engineering Science and Viscoelasticity: An Introduction*, Springer, 2010.

[4] L. C. EVANS, *Partial Differential Equations*, American Mathematical Society, 1998.

[5] J. A. FERREIRA, M. GRASSI, E. GUDINO, AND P. DE OLIVEIRA, *A 3D Model for Mechanistic Control of Drug Release*, SIAM Journal on Applied Mathematics, 74 (2014), pp. 620–633.

[6] J. A. FERREIRA, J. NAGHIPOOR, AND P. DE OLIVEIRA, *A coupled non-Fickian model of a cardiovascular drug delivery system*, Mathematical Medicine and Biology, (2015), pp. 1–29.

[7] J. A. FERREIRA, J. NAGHIPOOR, AND P. DE OLIVEIRA, *Analytical and numerical study of a coupled cardiovascular drug delivery model*, Journal of Computational and Applied Mathematics, 275 (2015), pp. 433–446.

[8] H. B. KELLER, *Approximation Methods for Nonlinear Problems with Application to Two-Point Boundary Value Problems*, Mathematics of Computation, 29 (1975), pp. 464–474.

[9] T. KHAMDAENG, J. LUO, J. VAPPOU, P. TERDTOON, AND E. E. KONOFAGOU, *Arterial stiffness identification of the human carotid artery using the stress-strain relationship in vivo.*, Ultrasonics, 52 (2012), pp. 402–411.

[10] S. MCGINTY, *A decade of modelling drug release from arterial stents.*, Mathematical biosciences, 257 (2014), pp. 80–90.

[11] S. MINISINI, *Mathematical and Numerical Modeling of Controlled drug release*, phd thesis, Politecnico di Milano, 2009.

[12] A. NEKOUZADEH, K. M. PRYSE, E. L. ELSON, AND G. M. GENIN, *A simplified approach to quasi-linear viscoelastic modeling.*, Journal of Biomechanics, 40 (2007), pp. 3070–3078.

[13] G. PONTRELLI AND F. DE MONTE, *A multi-layer porous wall model for coronary drug-eluting stents*, International Journal of Heat and Mass Transfer, 53 (2010), pp. 3629–3637.

[14] S. PRABHU AND S. HOSSAINY, *Modeling of degradation and drug release from a biodegradable stent coating.*, Journal of Biomedical Materials Research. Part A, 80 (2007), pp. 732–741.

[15] A. QUARTERONI AND A. VALLI, *Domain Decomposition Methods for Partial Differential Equations*, Numerical mathematics and scientific computation, Clarendon Press, 1999.

[16] F. ROSSI, T. CASALINI, E. RAFFA, M. MASI, AND G. PERALE, *Bioresorbable polymer coated drug eluting stent: A model study*, Molecular Pharmaceutics, 9 (2012), pp. 1898–1910.

[17] J. S. SOARES, *Constitutive Modeling for Biodegradable Polymers Application in Endovascular Stents*, phd thesis, Mechanical Engineering, Texas A&M University, 2008.

[18] X. ZHU AND R. D. BRAATZ, *A mechanistic model for drug release in PLGA biodegradable stent coatings coupled with polymer degradation and erosion*, Journal of Biomedical Materials Research Part A, 103 (2015), pp. 2269–2279.

[19] P. ZUNINO, *Multidimensional pharmacokinetic models applied to the design of drug-eluting stents*, Cardiovascular Engineering, 4 (2004), pp. 181–191.

Parameter/Variable	Definition	Value
	Stent coating	
$D_{W,S}^0$	diffusion coefficient of plasma	$10^{-8}\ cm^2/s$
$D_{O,S}^0$	diffusion coefficient of oligomers	$10^{-12}\ cm^2/s$
$D_{L,S}^0$	diffusion coefficient of lactic acid	$5 \times 10^{-12}\ cm^2/s$
$D_{DD,S}^0$	diffusion coefficient of dissolved drug	$5.7 \times 10^{-9}\ cm^2/s$
$k_{PW,S}$	rate of first reaction	$10^{-6}\ cm^2/g.s$
$k_{OW,S}$	rate of second reaction	$10^{-7}\ cm^2/g.s$
$k_{DD,S}$	dissolution rate	$10^{-5}\ mol/cm^2.s$
$\phi_{S,0}$	initial porosity	0
α	dimensional parameter	$1\ s/cm^2$
β	dimensional parameter	$10\ s/cm^2$
	Arterial wall	
$D_{W,V}$	diffusion coefficient of plasma	$10^{-8}\ cm^2/s$
$D_{O,V}$	diffusion coefficient of oligomers	$10^{-12}\ cm^2/s$
$D_{L,V}$	diffusion coefficient of lactic acid	$5 \times 10^{-12}\ cm^2/s$
$D_{D,V}$	diffusion coefficient of drug	$2.6 \times 10^{-9}\ cm^2/s$
D_σ	viscoelastic diffusion coefficient	$5 \times 10^{-10}\ g/(cmsPa)$
τ_1	relaxation time	$0.5\ s$
κ_r	Young's modulus	$4.1\ MPa$
κ_1	Young's modulus of the arm	$1\ MPa$
$k_{OW,V}$	rate of first reaction	$10^{-7}\ cm^2/g.s$
k_V	permeability of fluid	$2 \times 10^{-14}\ cm^2$
μ_V	viscosity of fluid	$7.2 \times 10^{-2}\ g/cm.s$
ϕ_V	porosity	0.61
γ	dimensional parameter	$10\ s/cm^2$
p_{lumen}	pressure in lumen	$120\ mmHg$
$p_{\mathrm{adv.}}$	pressure in adventitia	$30\ mmHg$

Table 1: Values of the parameters and variables in the stent coating and in the arterial wall.
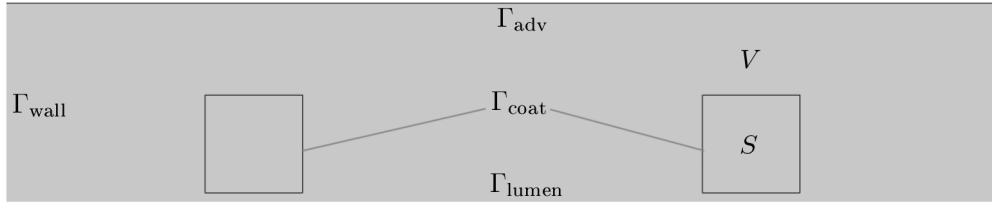
Figure 1: PLA based drug eluting stent, full-embedded in the arterial wall.
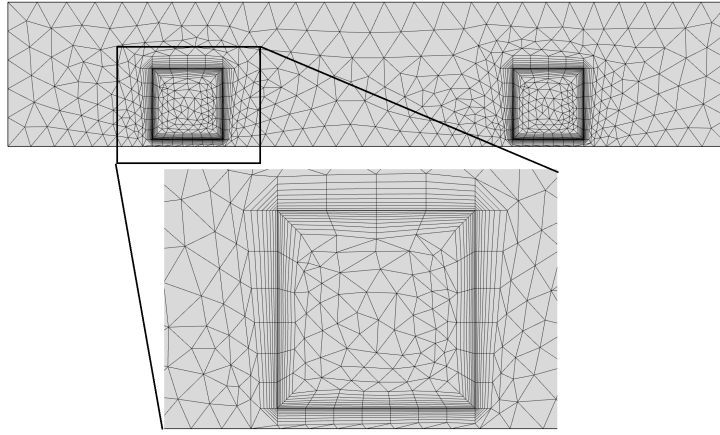
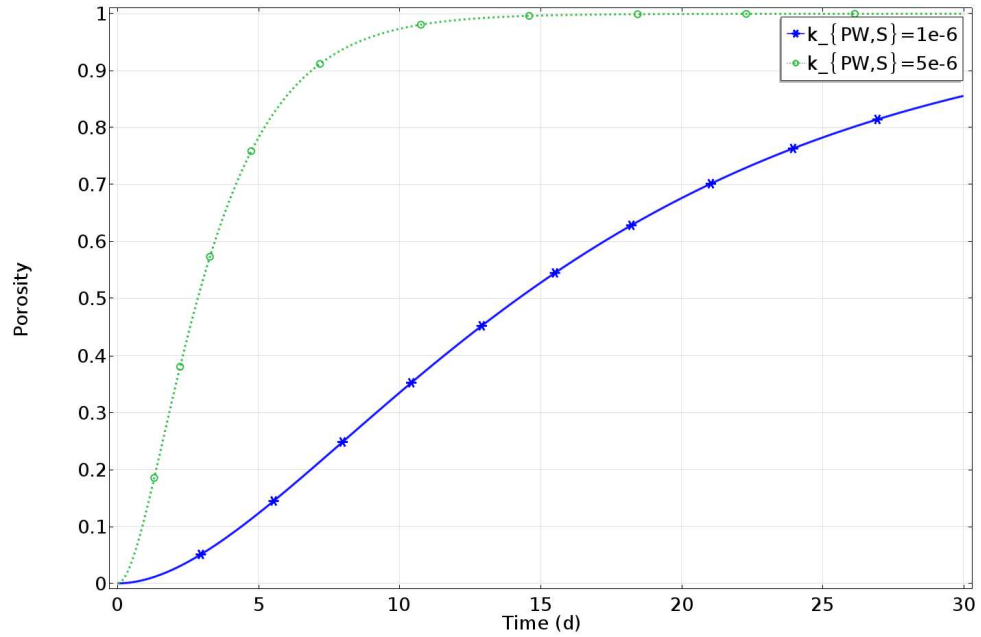Figure 2: Computational meshes in the domain.

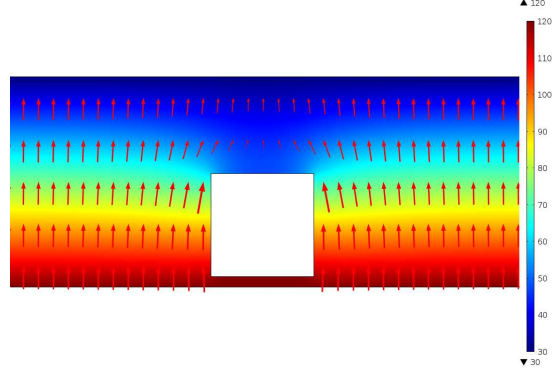Figure 3: The effect of degradation rate on the porosity of the polymer.

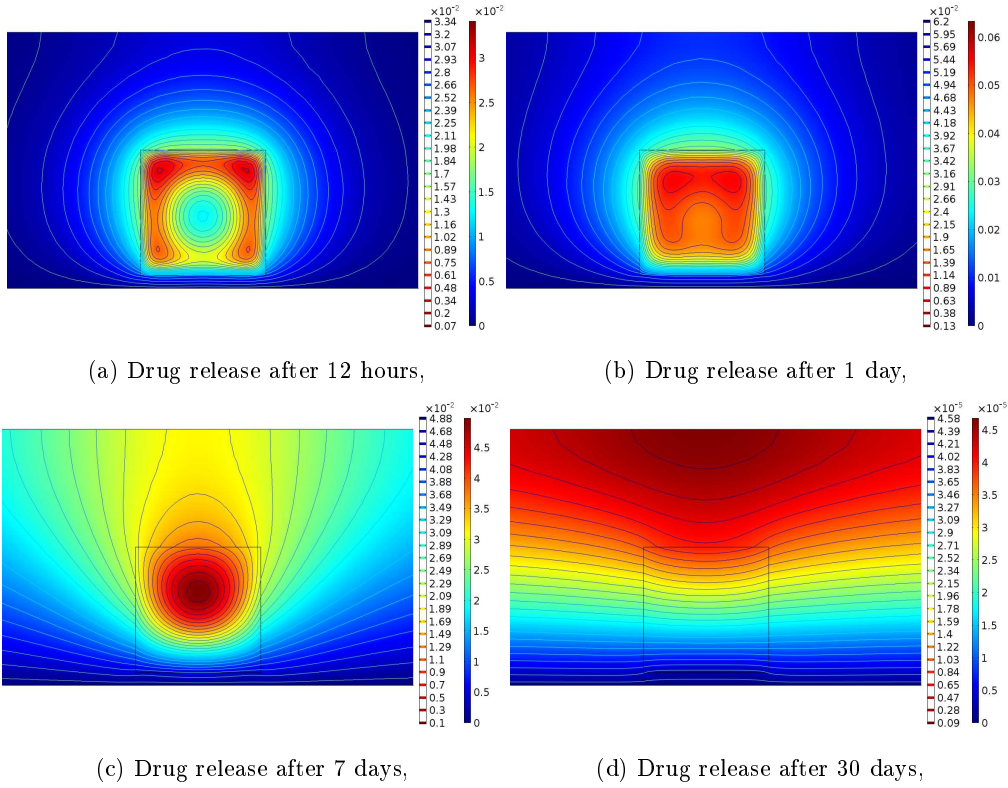Figure 4: Pressure distribution and velocity field in the stented arterial wall.

(a) Drug release after 12 hours,

(b) Drug release after 1 day,

(c) Drug release after 7 days,

(d) Drug release after 30 days,

Figure 5: Drug release from coating into the arterial wall during the first month, $k_{PW,S} = 10^{-6}$.
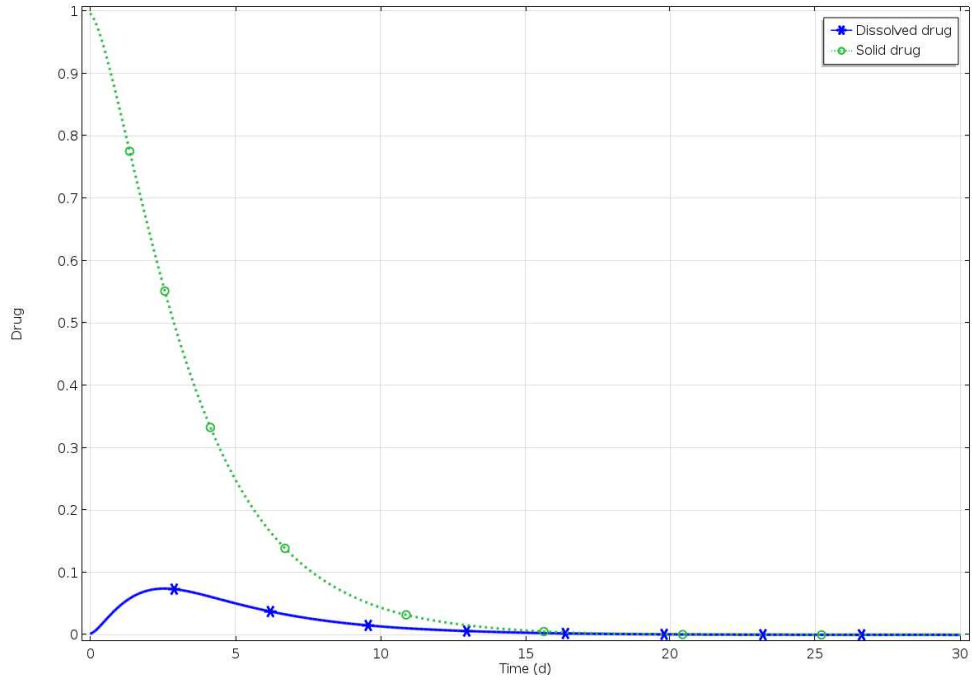
Figure 6: Dissolved and solid drugs in the stent during one month, $k_{DD,S} = 10^{-5}$.
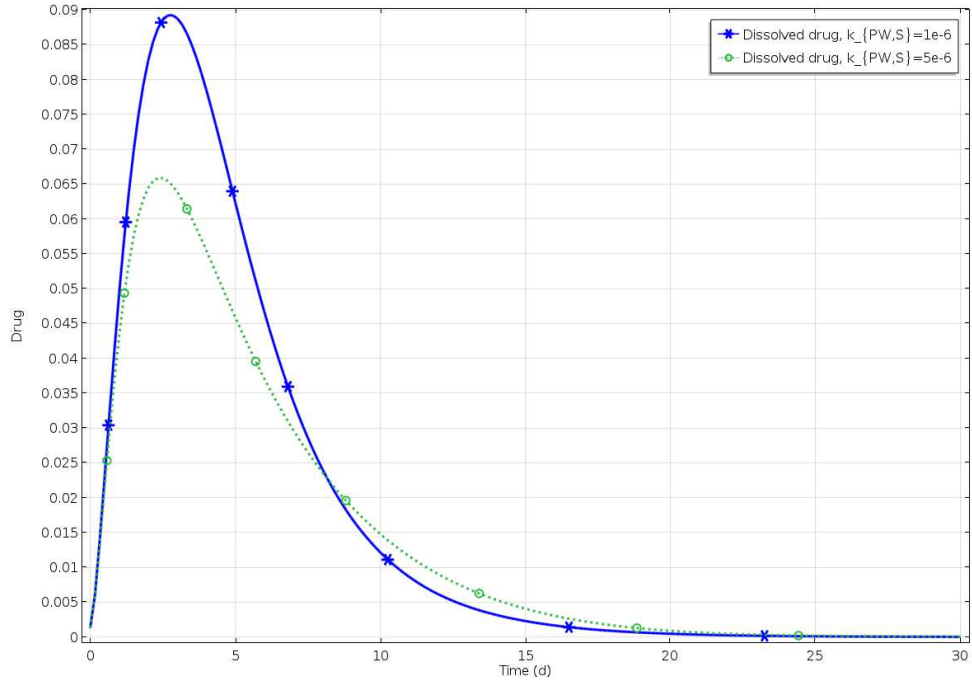
Figure 7: The effect of degradation rate on the drug accumulation in the stent.
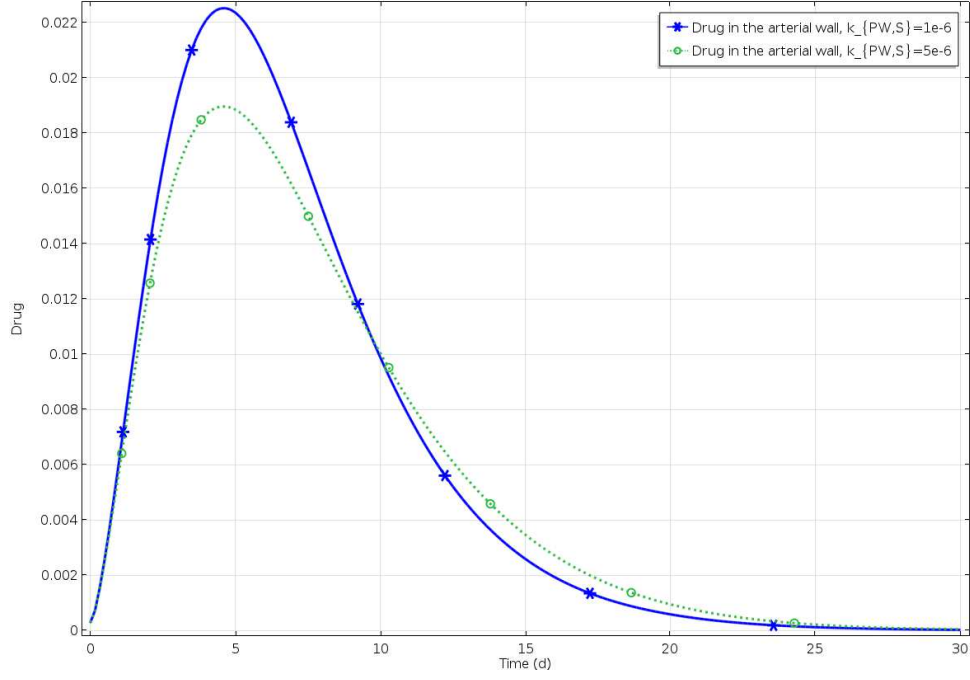
Figure 8: The effect of degradation rate on the drug accumulation in the arterial wall.
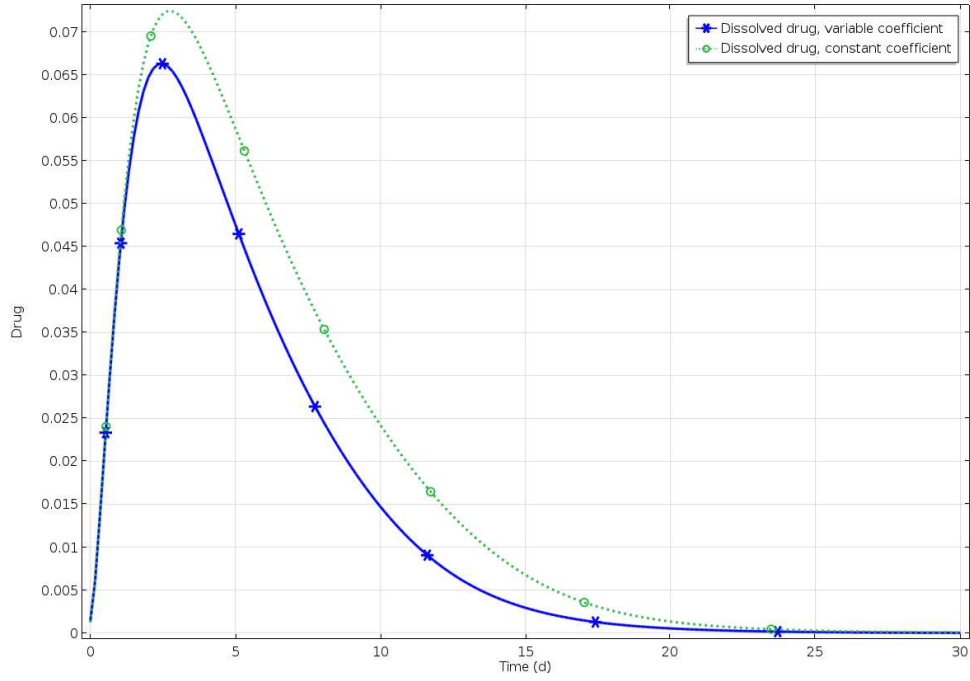
Figure 9: The effect of different diffusion coefficients on the accumulation of the dissolved drug in the stent, effective diffusion coefficient (3) versus constant diffusion coefficient $D_{DD,S}^0$, $k_{DD,S} = 10^{-5}$.
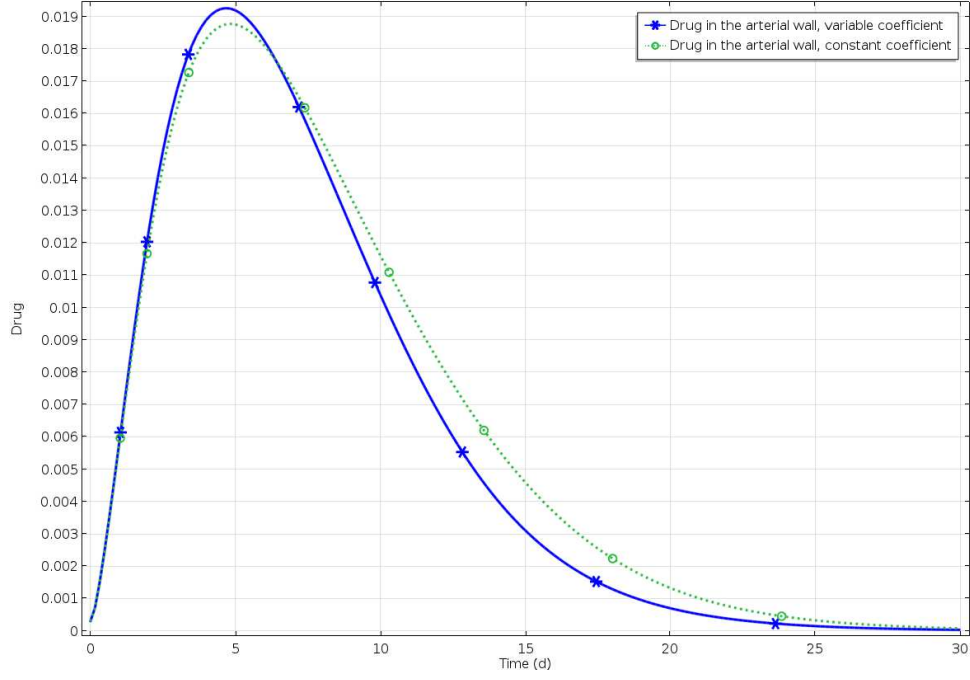
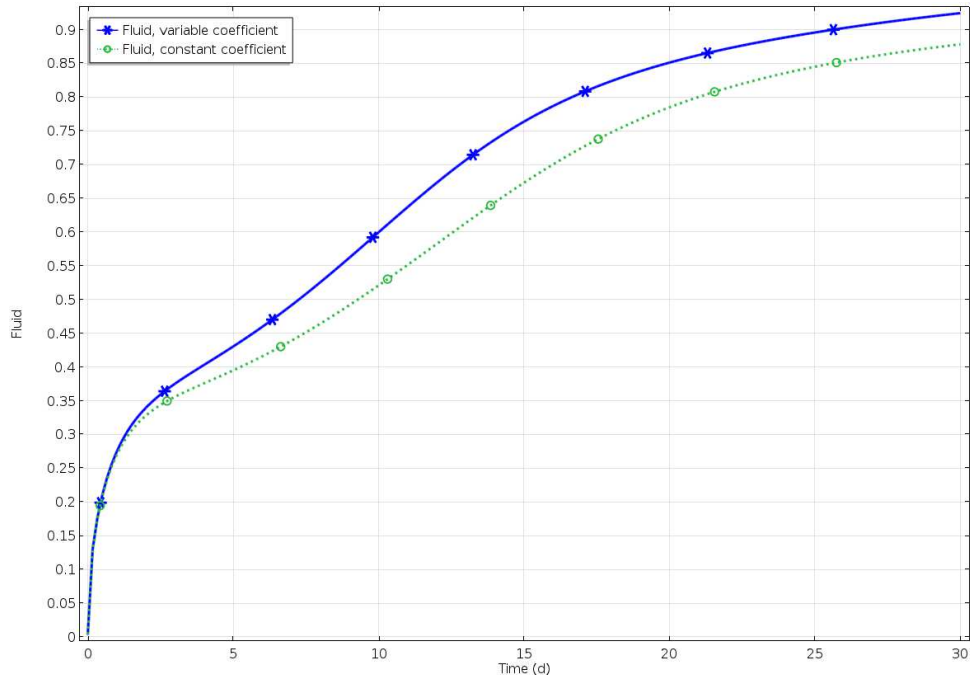Figure 10: The effect of different diffusion coefficients on the drug accumulation in the arterial wall, effective diffusion coefficient (3) versus constant diffusion coefficient $D_{DD,S}^0$, $k_{DD,S} = 10^{-5}$.

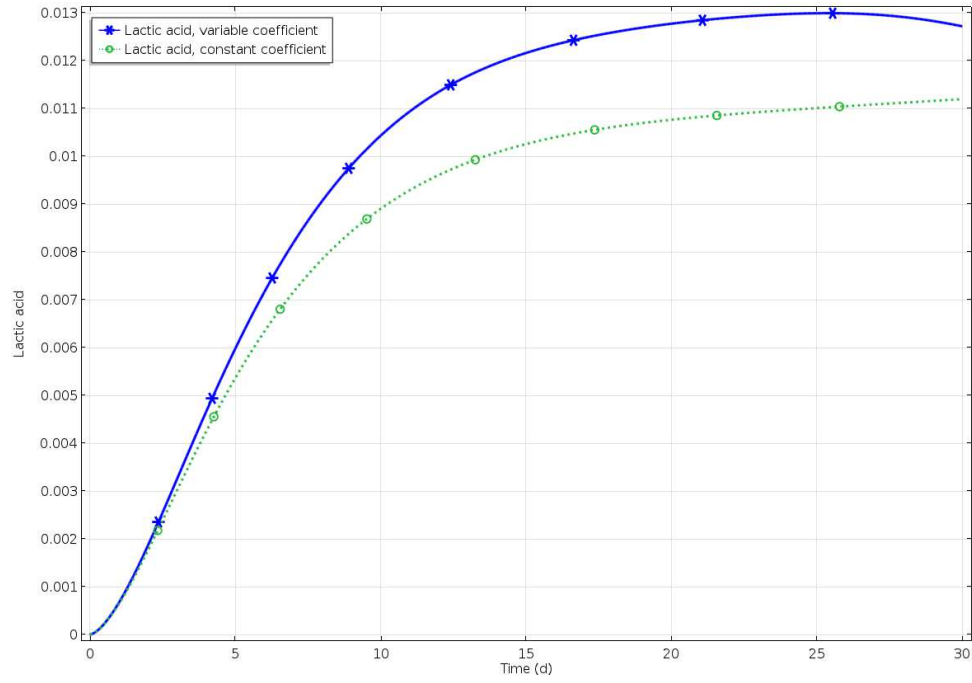Figure 11: The effect of different diffusion coefficients for the plasma in the stent.

Figure 12: The effect of variable diffusion coefficient on the lactic acid present in the arterial wall.
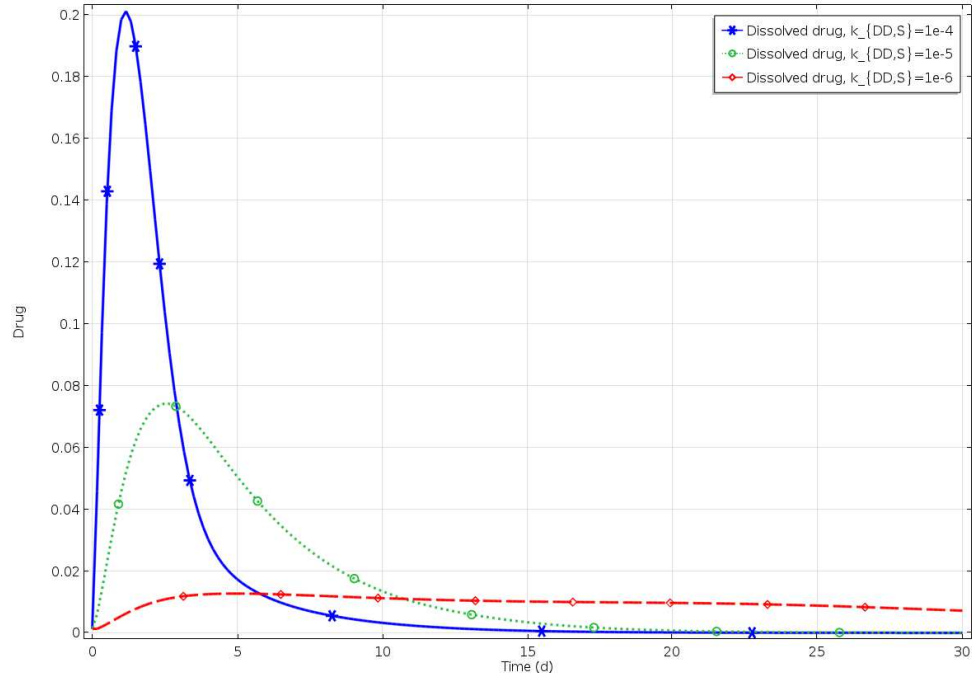

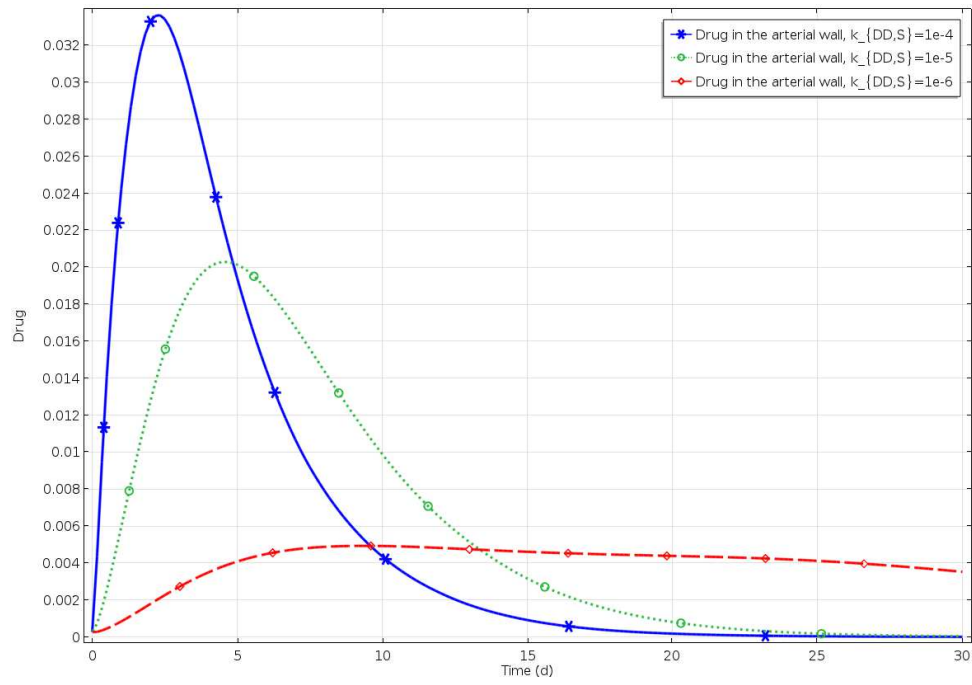Figure 13: The effect of dissolution rate on the drug accumulation in the stent.

Figure 14: The effect of dissolution rate on the drug accumulation in the arterial wall.